AFRL-SR-BL-TR-01-

0574

REPORT DOCUMENTATION PAGE

1. AGENCY USE ONLY *(Leave blank)*	2. REPORT DATE	3. REPORT TYPE AND DATES COVERED
	6/1/2001	Draft Final Report

4. TITLE AND SUBTITLE
Nanograin, Quasicrystalline, Multiphase Coatings for Reduced Friction and Wear

5. FUNDING NUMBERS
F49620-99-C-0067
STTR-TX

6. AUTHOR(S)
Fereydoon Namavar

7. PERFORMING ORGANIZATION NAME(S) AND ADDRESS(ES)
Spire Corporation
One Patriots Park
Bedford, MA 01730-2396

8. PERFORMING ORGANIZATION REPORT NUMBER
60423

9. SPONSORING/MONITORING AGENCY NAME(S) AND ADDRESS(ES
Air Force Office of Scientific Research
801 North Randolph St., Room 732
Arlington, VA 22203-1977

10. SPONSORING/MONITORING AGENCY REPORT NUMBER

11. SUPPLEMENTARY NOTES

12a. DISTRIBUTION/AVAILABILITY STATEMENT
APPROVED FOR PUBLIC RELEASE: DISTRIBUTION UNLIMITED

12b. DISTRIBUTION CODE

13. ABSTRACT *(Maximum 200 words)*

Recent progress in the development of quasicrystals (QCs) as low-friction, hard materials makes these alloys ideal candidates for protective coatings.

However one disadvantage of quasicrystals is that they are quite brittle. To overcome this problem, we are taking advantage of nanostructured materials and produce coatings which consist of a nanograin quasicrystals and metal.

Ultra smooth, nanograin Al-Cu-Fe-Cr and Al-Cu-Fe coatings with a nanohardness of 13 and 14 GPa respectively, were produced by Ion-beam assisted deposition (IBAD) and Pulsed laser Deposition (PLD) using targets prepared by the Materials Preparation Center at Ames Laboratory. Subsequent analysis by Ames Laboratory suggests that the coatings of Al-Cu-Fe-Cr produced are quasicrystalline in nature although an orthorhombic approximant cannot be ruled out by the data presented here.

Ultra smooth, nanograin Al-Cu-Fe thin films produced where substantially depleted in Al and enriched in Fe relative to the composition region in which quasicrystals can be produced in this system. However, nanohardness and x-ray data suggest that our AlCuFe coatings may be consist of quasicrystals of AlCuFe and iron alloys. Clearly additional work in Phase II is necessary to determine the appropriate conditions for producing quasicrystalline thin films of Al-Cu-Fe using the production method used.

14. SUBJECT TERMS

quasicrystals	hard coatings	nanostructure
wear-resistant	corrosion-resistant	
low-friction	multiphase	

15. NUMBER OF PAGES
30

16. PRICE CODE

17. SECURITY CLASSIFICATION OF REPORT	18. SECURITY CLASSIFICATION OF THIS PAGE	19. SECURITY CLASSIFICATION OF ABSTRACT	20. LIMITATION OF ABSTRACT
Unclassified	Unclassified	Unclassified	Unclassified

20011012 034

FR-60423

A Final Report for:

NANOGRAIN, QUASICRYSTALLINE, MULTIPHASE COATINGS FOR REDUCED FRICTION AND WEAR

Contract Period

15 September 1999 through 14 September 2000

Submitted under:

Contract No. F49620-99-C-0067

Submitted to:

Air Force Office of Scientific Research
AFOSR/NL ATTN: Major Paul Truelove
801 North Randolph Street, Room 732
Arlington, VA 22203-1977

Prepared by:

Fereydoon Namavar

Submitted by:

Spire Corporation
One Patriots Park
Bedford, MA 01730-2396

CLASSIFIED BY:

DECLASSIFY ON:

TABLE OF CONTENTS

LIST OF FIGURES

LIST OF TABLES

ABSTRACT

Recent progress in the development of quasicrystals (QCs) as low-friction, hard materials makes these alloys ideal candidates for protective coatings. Quasicrystal coatings can be substituted for some ceramics due to their high hardness and wear resistance, and lower-cost production. Their metallic nature may alleviate the adhesion problems associated with ceramic hard coatings on metallic substrates.

However one disadvantage of quasicrystals is that they are quite brittle. To overcome this problem, we are taking advantage of nanostructured materials and produce coatings which consist of a nanograin quasicrystals and metal. Multiphase nanograin materials generally exhibit higher hardness, toughness and increased ductility. The preferred deposition method is physical vapor deposition (PVD) with ion-beam bombardment. Combined PVD and ion beam is essential for controlling the grain size and increasing adhesion and film density. Therefore the objective of this program is to develop processes for fabrication of quasicrystal multiphase nanostructure layers to enhance toughness and reduce brittleness.

Ultra smooth, nanograin Al-Cu-Fe-Cr and Al-Cu-Fe coatings with a nanohardness of 13 and 14 GPa respectively, were produced by Ion-beam assisted deposition (IBAD) and Pulsed laser Deposition (PLD) using targets prepared by the Materials Preparation Center at Ames Laboratory. Subsequent analysis by Ames Laboratory suggests that the coatings of Al-Cu-Fe-Cr produced are quasicrystalline in nature although an orthorhombic approximant cannot be ruled out by the data presented here.

Ultra smooth, nanograin Al-Cu-Fe thin films produced where substantially depleted in Al and enriched in Fe relative to the composition region in which quasicrystals can be produced in this system. However, nanohardness and x-ray data suggest that our AlCuFe coatings may be consist of quasicrystals of AlCuFe and iron alloys. Clearly additional work in Phase II is necessary to determine the appropriate conditions for producing quasicrystalline thin films of Al-Cu-Fe using the production method used.

1. INTRODUCTION

Although much progress has been made in material processing techniques and in the development of new alloys, performance is still inadequate for some demanding applications. Additionally, in many other applications (e.g., where power transfer is an issue, such as the gearbox in gigantic machines), higher performance is desired, yet short-term development of new bulk materials or further improvements in existing alloys seems unlikely. In such cases, protective coatings can significantly improve performance. Coatings have become extremely important in applications where corrosion and wear resistance and low-friction are required, and there is great potential for advanced coating technologies to push forward the limit of performance of many current bulk materials. Loss of productivity and material due to friction and wear accounts for a few percent of the GNP of developed countries – in the hundreds of billions of dollars a year for the U.S. alone.

Improvements in surface properties by reducing friction, wear, and corrosion can be beneficial in two ways: extending the life of existing components, or increasing the load carrying capacity, or power density, of these components. The notion of reducing component size while maintaining load-bearing capability may be defined as "power density." Further improvements are now limited by bulk material properties, and can only be achieved by the implementation of new technologies such as advanced material coatings since conventional component lifetime improvement technologies such as material cleanliness, heat treatment, and hard finishing are mature.

The objective of this program is to develop a technology for deposition of adherent, hard, wear-resistant, oxidation-resistant, low-friction, nanostructured multiphase quasicrystalline coatings. The proposed coatings will fulfill a dual purpose: as ideal candidates for application in next-generation weapons systems, and as protective coatings for applications involving rolling, sliding, and mixed-mode contacts and in industries including biomaterials, transportation, and oil or geothermal well drilling.

2. QUASICRYSTALS

Quasicrystals are novel materials, typically composed of three or more metals, discovered in 1982.[1] While conventional crystals are constructed of a single type of building block, for example a cube, quasicrystals are not.[2-4] Yet, quasicrystals exhibit characteristics common to crystals. Quasicrystals appear to be built with an order to them but their building blocks are organized in an aperiodic rather than periodic (repeating) fashion. Quasicrystals are known for being hard, slippery, poor conductors of heat, and resistant to attack by chemicals.[5,6] The properties of quasicrystals are particularly useful for applications requiring high hardness, resistance to wear, low adhesion or a barrier to elevated temperatures.[6-9] One disadvantage of quasicrystals is that in bulk form they are quite brittle. Hence, we focus in this work on producing coatings of these materials designed to reduce their brittleness and yield an exceptionally hard coating, thus eliminating a barrier to their usefulness.

While materials that form quasicrystals are relatively abundant, producing these materials is non-trivial because they form in very narrow composition ranges. The vast majority of quasicrystals discovered to date contain aluminum as their major component. Of the aluminum-based materials, the most commercially viable are those containing aluminum, copper, and iron because of the relatively low cost of the elements used. Typical properties of these materials in comparison to more common materials are shown in Table 1.

Table 1 **Typical Physical and Mechanical Properties of Al-Cu-Fe and Al-Cu-Fe-Cr Compared to Common Benchmark Materials**

Property	Value	Material
Hardness (Hv)	6000-10000	diamond[15]
	750-1200	silica[15,16]
	470-1000	qc Al-Cu-Fe[6,11,17,18]
	400-720	Al-Cu-Fe-Cr[6,11,14]
	70-200	low-carbon steel[15,16]
Coefficient of friction	0.32	low-carbon steel[19]
	0.05-0.2	qc Al-Cu-Fe[6,19]
	0.06-0.2	Al-Cu-Fe-Cr[6,20]
Fracture toughness (MPa $m^{1/2}$)	1.5	silica[21]
	1	qc Al-Cu-Fe[17,18]
Thermal Conductivity (W m-1 K-1) at RT	50	low-carbon steel[22]
	2	yttria-doped zirconia[17]
	1.8	qc Al-Cu-Fe[17]
	1.7	qc Al-Cu-Fe-Cr[23]

Al-Cu-Fe-Cr in particular is known to be particularly resistant to corrosion because of the addition of Cr.[10,11] Furthermore, there are several approximant phases near the quasicrystalline region of the phase diagram of Al-Cu-Fe-Cr. An approximant is a material that is crystalline but is composed of large building blocks (unit cells) with aperiodic motifs.[12] For example, for the Al-Cu-Fe-Cr system, these building blocks can be on the order of 24Å x 12Å x 32Å.[7] These approximants are known to have properties similar to that of the quasicrystalline material. Thus, from an industrial point of view, making materials with the interesting properties of quasicrystals is easier with a material with approximant regions surrounding the narrow quasicrystalline phase field. The phase field for Al-Cu-Fe-Cr that includes both the quasicrystalline and approximant regions encompasses at least $Al_{64.6\text{-}75}Cu_{4.5\text{-}20.5}Fe_{5.0\text{-}13.0}Cr_{2.1\text{-}18.5}$ according to early work.[7] By comparison, Al-Cu-Fe forms a quasicrystalline phase in a region of $Al_{61.5\text{-}65}Cu_{23\text{-}30}Fe_{9\text{-}13}$.[13]

The best-known quasicrystalline product to date is commercial cookware coated by thermal spraying with quasicrystalline $Al_{70.5}Cu_{10.0}Fe_{8.8}Cr_{10.7}$, a.k.a. Cybernox®.[14] One problem with thermal spraying such coatings is that the results yield coatings that are very rough,[14] thus requiring polishing if useful features such as good wear properties and low friction are to be exploited.[6,14] In addition, these coatings are quite porous, which can be a problem for some applications, and porosity can affect the materials properties. Developing a method to make smoother films without polishing and reducing porosity could be quite advantageous.

2.1 Experimental procedures

During this program we have studied production of quasicrystalline AlCuFe and AlCuFeCr by ion-beam assisted deposition (IBAD) and pulsed laser deposition (PLD) respectively. As mentioned before, Ames Laboratory provided source materials. The quasicrystalline $Al_{71.0}Cu_{10.0}Fe_{8.5}Cr_{10.5}$ alloy system has been also deposited by thermal spray at Ames Laboratory for comparing their hardness and roughness with our coatings.

Immediately after each coating run, samples were sent to Ames Lab for characterization and analysis. However, we have also performed measurements such as Rutherford backscattering spectroscopy (RBS), microhardness, nanohardness, and transmission electron microscopy (TEM) to determine mechanical and material properties of our coatings.

2.1.1 *Target Preparation*

Al-Cu-Fe-Cr: Our collaborators at Ames Laboratory are pioneers in the quasicrystal field. Source (bulk) materials have been produced at Ames Laboratory. Target preparation involved the production of $Al_{71.0}Cu_{10.0}Fe_{8.5}Cr_{10.5}$ powder at Ames Laboratory via high-pressure gas atomization.[24] The highest purity elements available were used to produce this powder. Gas atomization yielded spherical powder particles with a size $\leq$ 10μm. The powder was then sintered at 800°C under vacuum for 4 hours. After sintering the material was then sealed into an evacuated (~10mTorr) stainless steel can and hot isostatically pressed (HIPed). During the HIPing process the temperature was first ramped up to 400°C, and a pressure of 45,000 psi was applied. Next, the sample was heated to 800°C while under pressure and held for 2 hours. Finally, the unit was cooled and depressurized. X-ray diffraction (XRD) indicated that these targets (DJS-10-93-B) were quasicrystalline or a related approximant. See Figure 1. As discussed in the introduction, the orthorhombic approximant cannot be distinguished from the quasicrystal phase of Al-Cu-Fe-Cr by XRD. However, the properties of these materials are very similar and thus such a distinction, which can only be made by TEM, was not deemed necessary. XRD was accomplished using a Phillips spectrometer with a Cu Kα anode operating at a 40 kV accelerating voltage and 20 mA beam current.

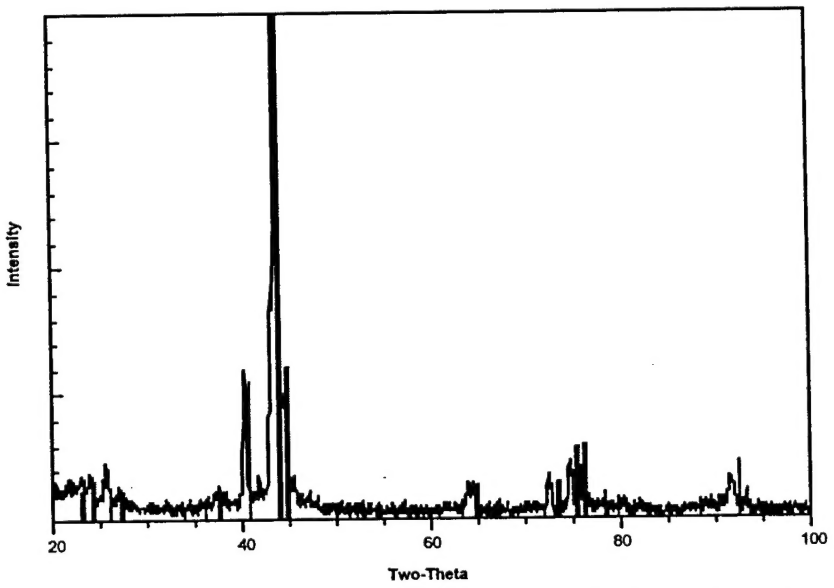

Figure 1 **XRD (XRD 11874) results for Al-Cu-Fe-Cr target (DJS-10-93-B). Bars represent literature XRD results for decagonal Al-Cu-Fe-Cr.[25]**

After production and receipt of these materials from Ames Laboratory, we used them in our evaporation. After deposition of nanocrystalline quasicrystal coatings and preliminary analysis at Spire, selected samples have been sent to Ames Laboratory for further evaluation.

(Al-Cu-Fe): The first target produced by HIP by Ames Laboratory was an icosahedral quasicrystalline sample of nominally $Al_{63}Cu_{25}Fe_{12}$. Like the Al-Cu-Fe-Cr samples this was prepared by first producing powder by gas atomization and subsequently HIPing the powder.

The second sample produced by Ames Laboratory was arc-melted coupons of composition $Al_{40}Cu_5Fe_{55}$. Specifically, these coupons were made from > 99.99% pure elements by arcmelting on a water-cooled copper hearth plate in an atmosphere of argon. This composition was chosen based upon published reports by researchers in Japan about the use of

electron beam evaporation to produce quasicrystalline thin films[26]. A decreased amount of Al and Cu in the targets relative to the desired quasicrystalline composition of $Al_{63}Cu_{25}Fe_{12}$ is necessary to produce quasicrystalline films via this method because of the high vapor pressure of Al and Cu relative to Fe. In addition, if ion beams are used to produce films one have to be careful because preferential sputtering of Al is known to occur.[27]

2.2 Ion-beam assisted deposition (IBAD)

IBAD combines evaporation with concurrent ion beam bombardment in a high vacuum environment as shown schematically in Figure 2. Typically, base pressure is about $< 10^{-7}$ torr and the operating pressure is $< 10^{-5}$ torr. A vapor flux of atoms is generated with an electron beam evaporator and deposited on a substrate. Typically, ions of a particular gas are simultaneously extracted from a plasma and accelerated into the growing film at energies of several hundred to several thousand electron volts (eV).

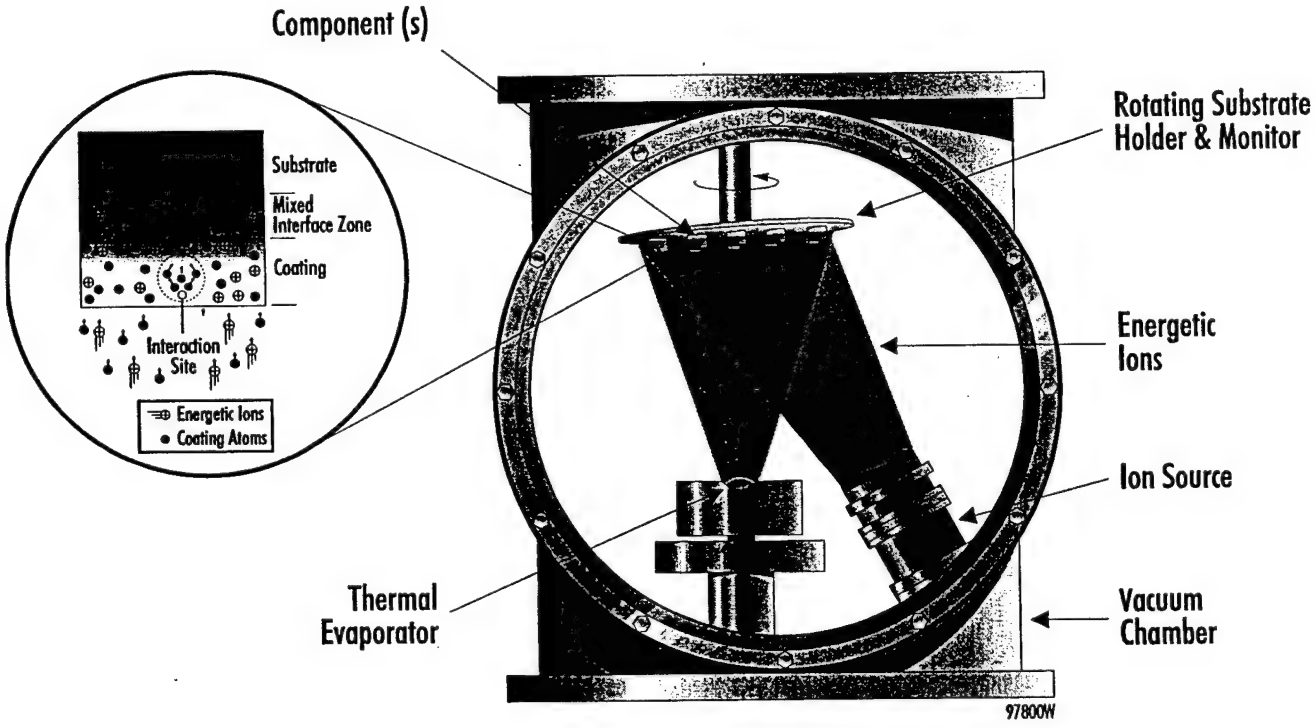

Figure 2 **Schematic of IBAD process. The process combines physical vapor deposition (evaporation) with concurrent ion beam bombardment to produce a wide range of coatings with exceptional adhesion to virtually any substrate.**

Ion bombardment is the key factor in controlling film properties in the IBAD process. It is crucial for improving adhesion, morphology, density, stress level, crystallinity, and chemical composition. IBAD enhances adhesion in a number of ways, by: (1) removing contaminant layers, (2) increasing substrate/coating atom reactivity, (3) generating a microscopically rough surface, (4) increasing nucleation density, (5) increasing surface mobility of coating atoms, (6) decreasing formation of interfacial voids, and (7) introducing thermal energy to the surface region. The columnar microstructure often observed in low-temperature conventional PVD (physical vapor deposition) film growth can be eliminated through sputtering and redeposition, increased nucleation density, and increased surface mobility of coating atoms. Chemical properties of the surface can be influenced, if desired, by using reactive ion species during the IBAD process. The outstanding control over film properties inherent in the IBAD process is

created by the flexibility one has in selecting evaporation source, evaporation rate, ion species, ion energy, and ion beam current density.

2.3 Pulsed laser Deposition (PLD)

Since 1985 PLD has become a very active area of materials research.[28] Thin films of a large number of different materials have been grown via this unique process. One drawback of both electron-beam evaporation and sputtering lies in the reproducibility in obtaining the proper film stoichiometry of the complex chemical compounds. In the case of electron-beam evaporation the constituents of a binary or ternary alloy will evaporate at radically different rates due to differences in the individual vapor pressures of the alloy constituents.

The unique nature of PLD, on the other hand, provides a PVD technique that readily replicates the target stoichiometry of most multi-component materials. This is due to the fact that the laser ablation process is essentially a flash evaporation of a small volume of the target material in a very short time (~20 ns). During this non-linear thermal process essentially 100% of a small section of the target is instantly vaporized in a time frame that differences in the individual vapor pressures' of the various target elements becomes irrelevant. In this way then, the re-condensed ablated material reforms on the substrate as a thin film with the correct target stoichiometry. The ablation plume consists of ground state and excited atoms and molecules, as well as ions, radicals, and particulates.

2.3.1 Experimental Results

Al-Cu-Fe-Cr produced by PLD: Al-Cu-Fe-Cr was deposited onto a silicon wafer by use of an excimer laser operating at 248 nm (KrF), delivering ~500 mJ per pulse at a repetition rate of 50 Hz. (See Figure 3). Samples were studied by energy dispersive spectroscopy (EDS) at Northwestern University and Ames Laboratory. Table 2 shows results for AlCuFeCr source and coated materials. Ames Lab measured a composition (in atomic %) of $Al_{62.6}Cu_{12.7}Fe_{10.8}Cr_{13.9}$ for as deposited PLD sample. In comparison, results from Northwestern University showed a target bulk composition of $Al_{71.1}Cu_{9.0}Fe_{8.2}Cr_{11.7}$ and a film composition of $Al_{73.9}Cu_{8.5}Fe_{7.3}Cr_{10.4}$. Discrepancies can arise between EDS results produced from different instruments because EDS relies on the use of sensitivity factors and different instruments may use different sensitivity factors to calculate compositions. Rutherford backscattering (RBS) results by Charles Evans and Associates (Figure 4) indicate a surface composition (for the annealed thin film) of $Al_{66.4}Cu_{11}Fe_{9.6}Cr_{13.0}$ which is in closer agreement to that observed by Northwestern University than results obtained by Ames Lab.

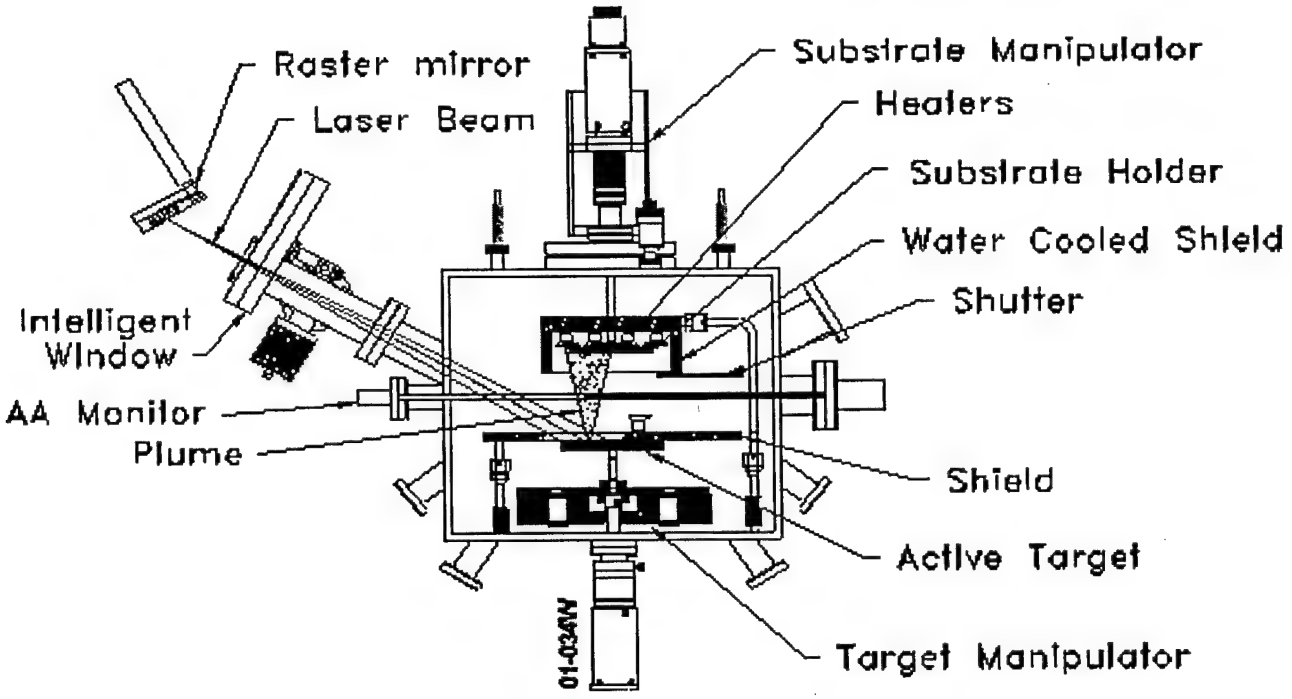

Figure 3 **Schematic of PLD process using an excimer laser operating at 248 nm (KrF), delivering ~500 mJ per pulse at a repetition rate of 50 Hz**

Table 2 **Composition of AlCuFeCr Coating produce by PLD.**

	Lab	Methods	Heath Treatment	Al Atomic %	Cu Atomic %	Fe Atomic %	Cr Atomic %
Source Materials AlCuFeCr	Ames	Nominal Values	No	71.0	10.0	8.5	10.5
Source Materials AlCuFeCr	NW	EDS	No	71.07	9.04	8.15	11.74
Coating AlCuFeCr On Si	NW	EDS	No	73.79	8.49	7.31	10.42
Coating AlCuFeCr On Si	Ames	EDS	No	62.6	12.7	10.8	13.9
Coating AlCuFeCr On Si	Ames	EDS	500°C	63.7	11.2	10.9	14.2
Coating AlCuFeCr On Si		RBS	500°C	66.4	11.0	9.6	13.0

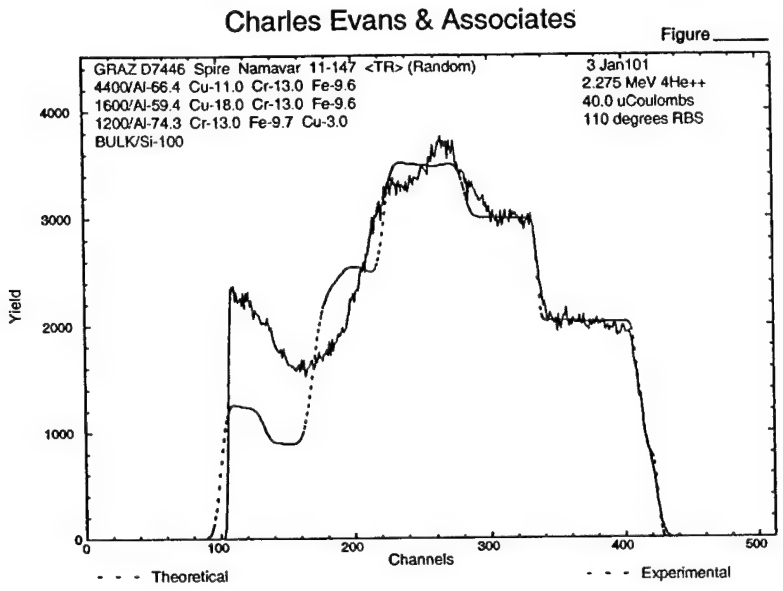

Figure 4 **2.275 MeV RBS spectra for Al-Cu-Fe-Cr on Si by PLD process after annealing (black solid line) and theoretical models (red dotted line). The composition of near surface layer is $Al_{66.4}Cu_{11}Fe_{9.6}Cr_{13}$.**

Since as deposited thin films of Al-Cu-Fe-Cr did not show any evidence of quasicrystalline (QC) structures by XRD; therefore, we subsequently annealed the Al-Cu-Fe-Cr sample at 300°C for 1 hour under vacuum. We found no evidence of quasicrystallinity by XRD, as shown in Figure 5a. However, once annealed at 500°C for 1 hour we found evidence of quasicrystallinity by XRD and an unidentified phase, possibly the cubic phase of Al-Cu-Fe-Cr, as show in Figure 5b. For many methods of film production an annealing step has been found necessary to yield a quasicrystalline film[29] so the requirement for annealing our films is not surprising. Table 3 shows the expected peak locations and the observed locations for all three heat treatment conditions of this coating.

2.3.2 TEM Analysis of AlCuFeCr Films produced by PLD

X-ray diffraction (Figure 6) of the as deposited coating indicates that the coating is consist of very fine-grained materials. In fact the presence of fine grains in as deposited Al-Cu-Fe-Cr confirmed by TEM analysis (Figure 7). The bright spots in the dark field TEM images (Figure 7a) show grains as large as 10 nm for the as-deposited sample. Selected area diffraction (SAD) from the as-deposited sample showed continuous rings indicative of a small grain size. Use of the smallest aperture also showed continuous rings, which is a characteristic of polycrystalline materials. (As we will discuss SAD for annealed Al-Cu-Fe-Cr sample using same small aperture provide a pattern, which typically observed for single crystal/QC materials See Figure 8). The surface of these samples is extremely smooth. Indeed, surface profilometry results (Figure 9) determined at Ames Laboratory for Al-Cu-Fe-Cr coatings indicate the roughness of the films below limit of detection of their system suggesting, Al-Cu-Fe-Cr samples produced by plasma spray at Ames Laboratory, several order magnitude rougher than of a coating produced by Spire

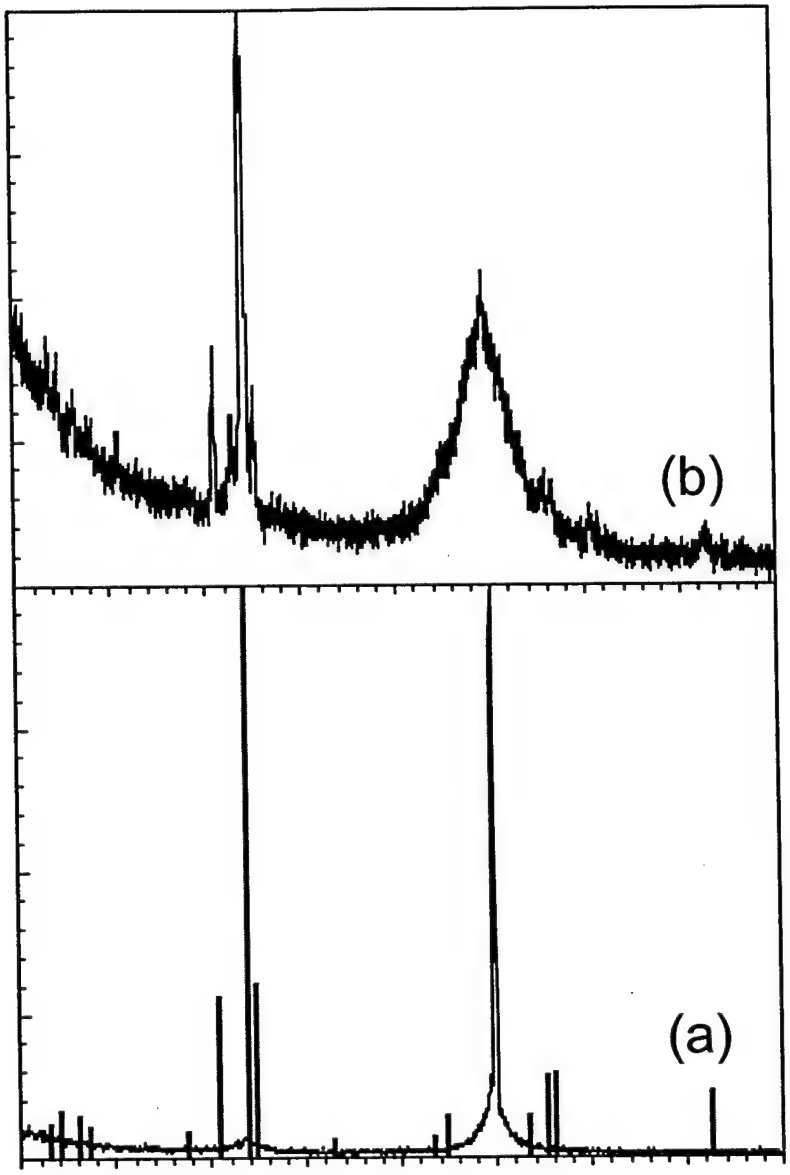

Figure 5 (a) XRD results for thin films of PLD Al-Cu-Fe-Cr heated at 300°C and (b) XRD results for thin films of Al-Cu-Fe-Cr heated at 500°C. Bars represent literature XRD results for decagonal Al-Cu-Fe-Cr.[25]

Table 3 **Tabulated XRD results for the Al-Cu-Fe-Cr thin films and literature values for decagonal Al-Cu-Fe-Cr.**

2*Theta	Relative Intensity As-Deposited	Relative Intensity After heat treating at 500°C for 1 hour	Relative Intensity Literature Results for Decagonal Al-Cu-Fe-Cr[25]
23.10			0.060
23.58		0.408	
24.24			0.083
24.58		0.384	
26.05			0.070
26.30		0.340	
27.30			0.053
30.82		0.266	
37.60			0.045
40.70			0.281
41.02		0.417	
42.88		0.267	
42.95	0.781		
44.00			1.000
44.10		1.000	
44.80			0.305
45.16		0.347	
52.65			0.031
63.25			0.034
64.75			0.070
68.95	1.000		
69.37		0.509	
73.45			0.073
75.40			0.142
75.60		0.176	
76.15			0.147
76.45			
92.50			0.115
92.60		0.080	

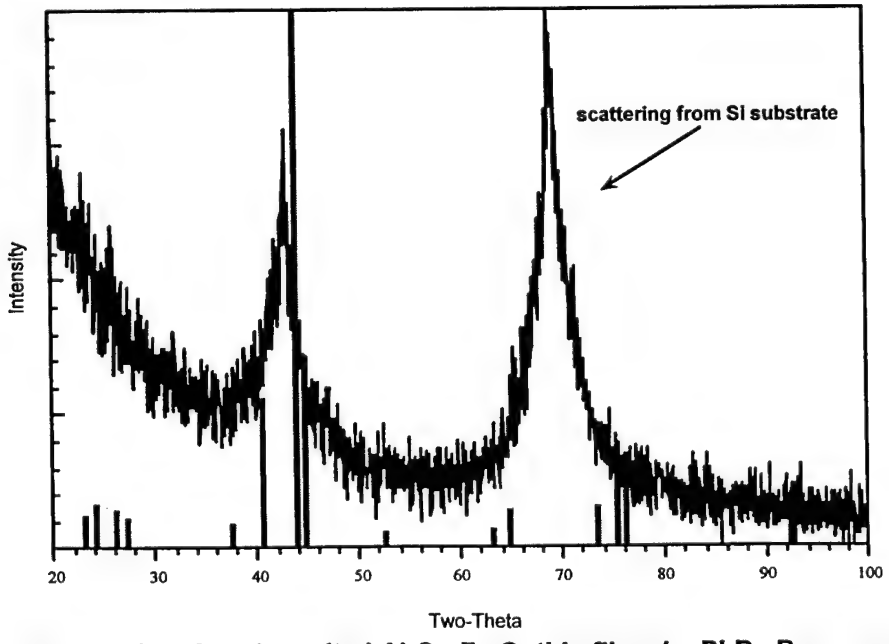

Figure 6 **XRD results of as-deposited Al-Cu-Fe-Cr thin films by PLD. Bars represent literature XRD results for decagonal Al-Cu-Fe-Cr.[25]**

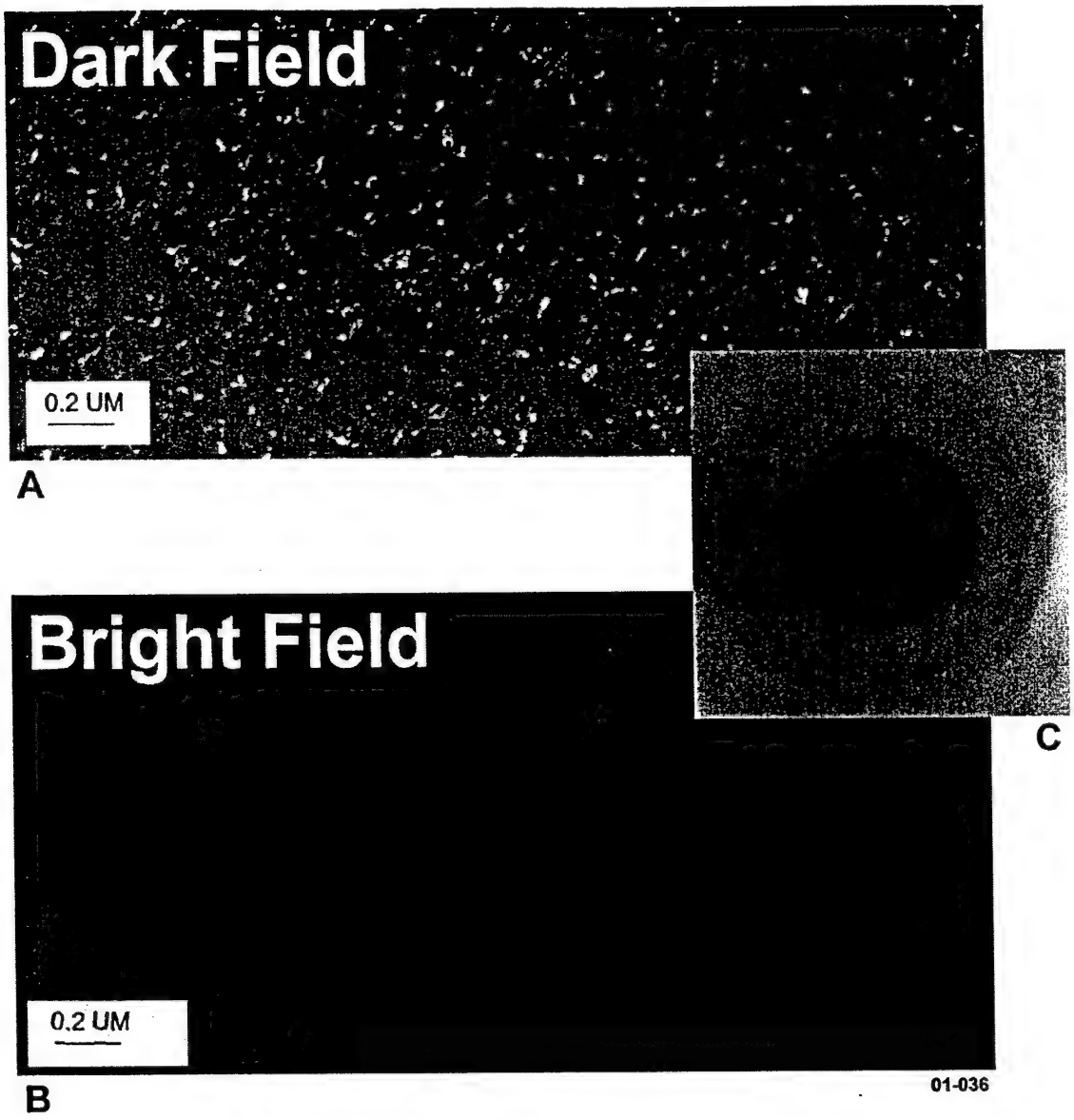

Figure 7 **Typical plane view transmission electron microscopy for AlCuFeCr produced by PLD. (a) Dark field image shows AlCuFeCr nanograins with dimensions of about 10 nm. (b) Bright field image shows that PLD AlCuFeCr has a very smooth surface (c) Diffraction pattern for surface shows continuous rings indicative of a small grain size.**

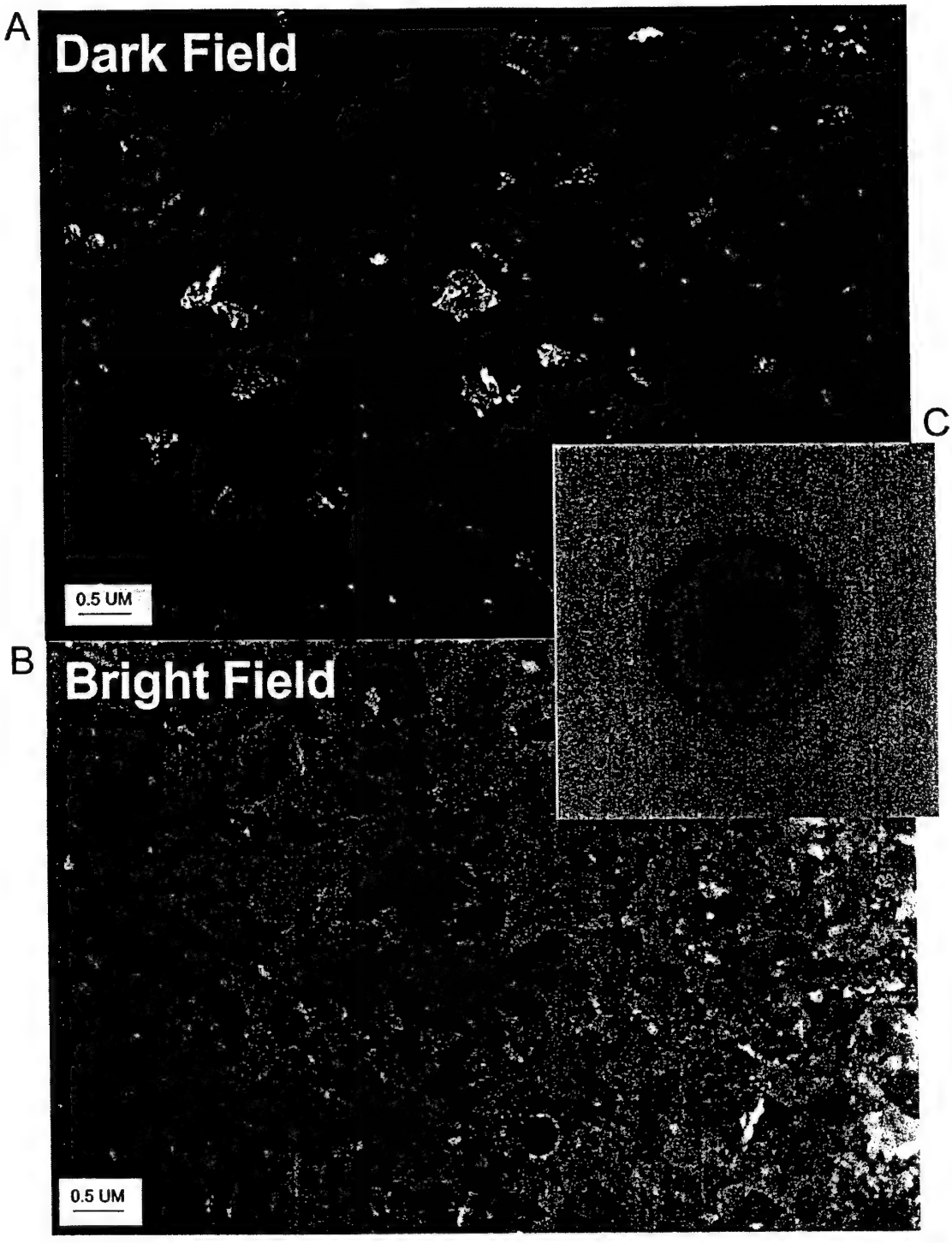

Figure 8 **Typical plane view transmission electron microscopy for annealed (500°C) AlCuFeCr produced by PLD. (a) Dark field image shows AlCuFeCr nanograins with dimensions of about 100-500 nm. (b) Bright field image (c) Electron diffraction pattern using a large (several microns diameter) aperture. (Concluded on following page.)**

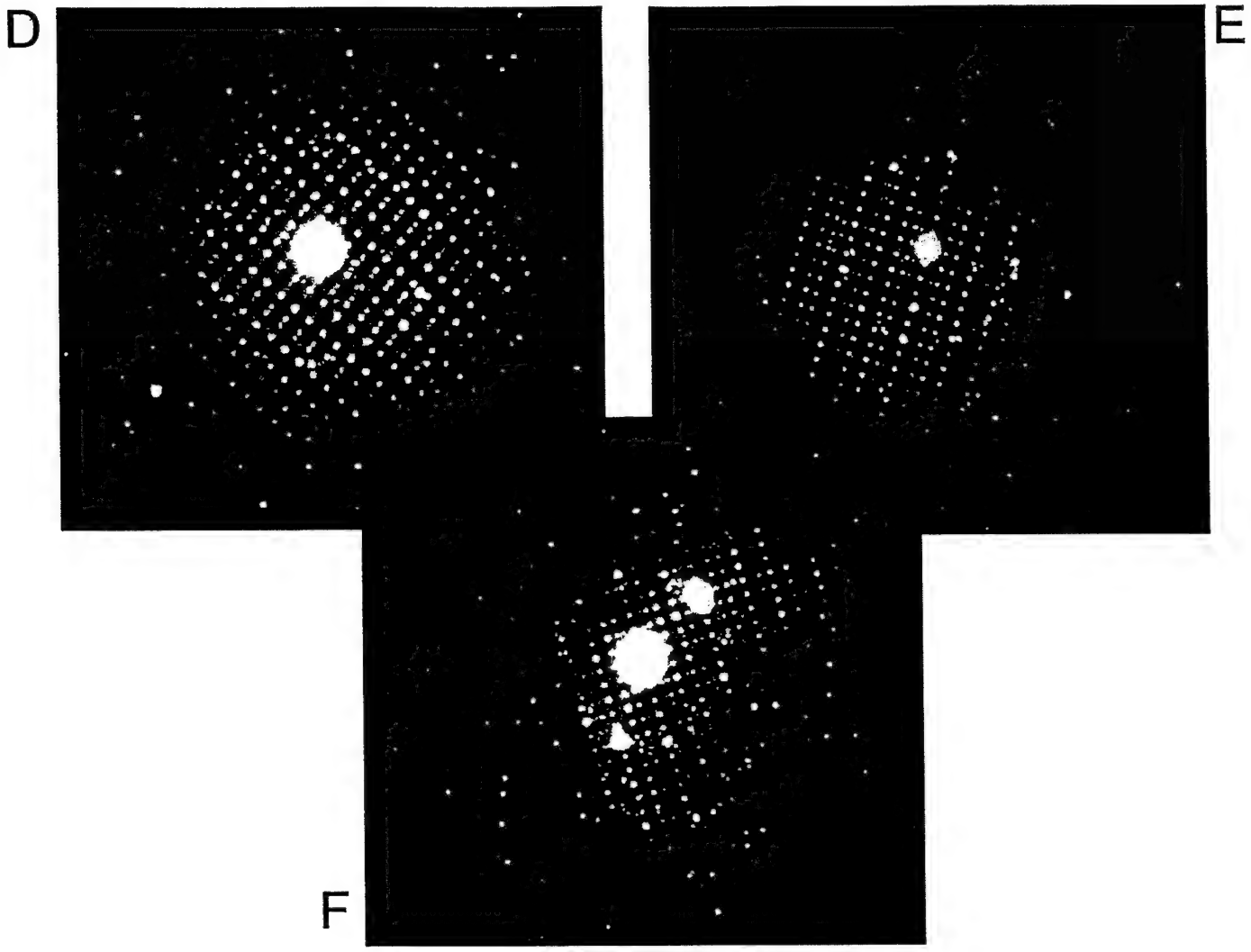

Figure 8 (concluded) **(d), (e) and (f) Electron diffraction patterns using a small (about half micron diameter) aperture showing single crystal patterns for different individual grains.**

Figure 8 shows plane view transmission electron microscopy (TEM) for annealed (500°C) Al-Cu-Fe-Cr produced by PLD. The dark-field TEM image of the coating shows 100 to 1000 nm grains. The bright spots show only the diffracting Al-Cu-Fe-Cr (Figure 8a) nanocrystals, which are oriented about a certain direction. Therefore, the grain size measurement becomes very accurate. Figure 8c shows an electron diffraction pattern using an aperture with dimensions of several microns diffracting from a large number of grains. This pattern is similar to those of polycrystalline materials. Figure 8d, 8e, and 8f show selected area diffraction patterns using an aperture with dimension of a half micron demonstrating single crystal patterns for different individual grains of Al-Cu-Fe-Cr.

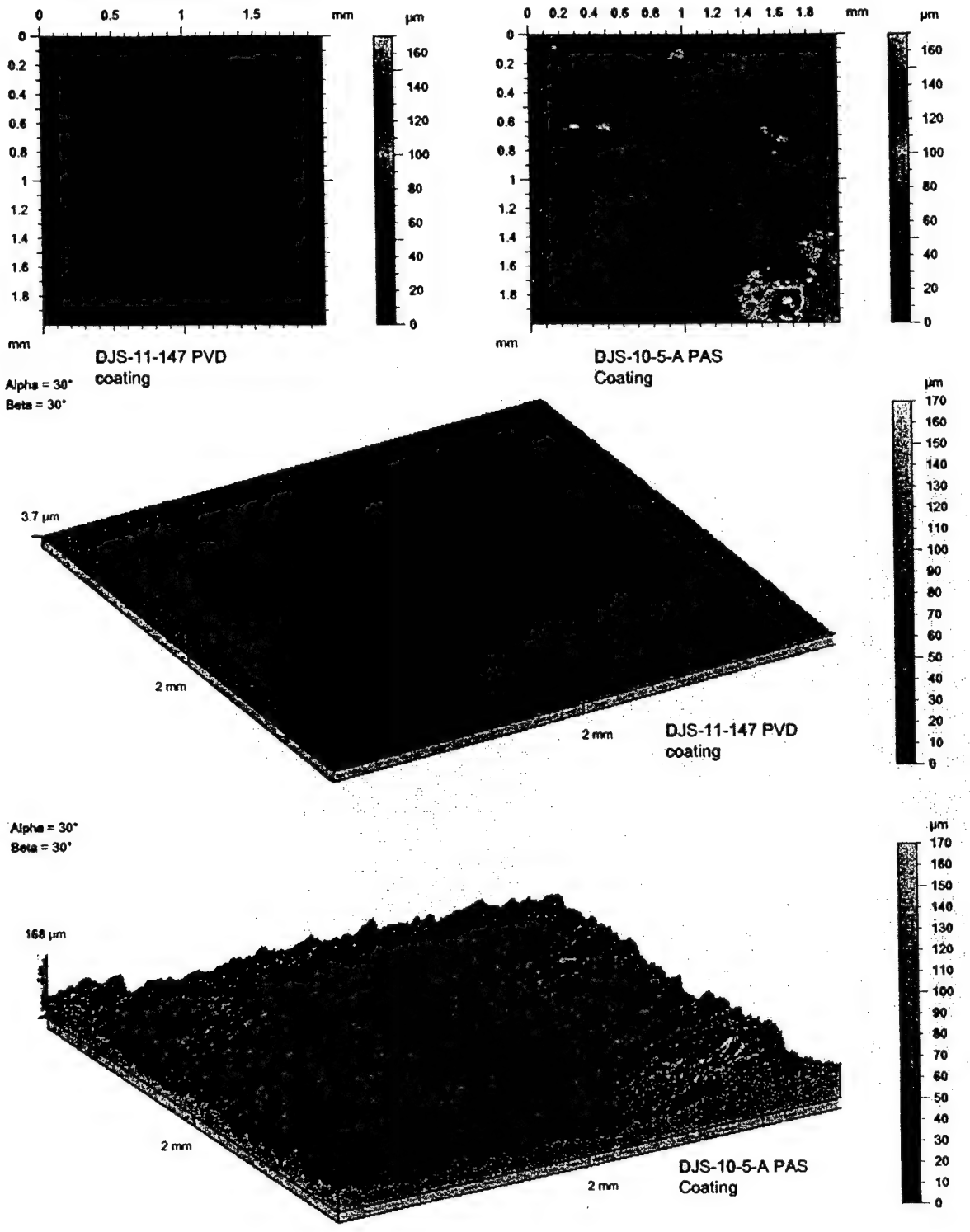

Figure 9 **Surface profilometry results for Al-Cu-Fe-Cr coatings showing the roughness of the films. (upper left) top view of a coating produced by PLD, (upper right) top view of an Al-Cu-Fe-Cr produced by plasma spray at Ames Laboratory, (middle) tilted view of a coating produced by Spire and (bottom) tilted view of a coating produced by plasma spray. Note the scale of the middle and bottom figure.**

These figures are strongly suggestive of quasicrystallinity. Note, in particular, the periodic spacing of spots in one direction (all spots equally spaced) and the apparent aperiodic (unequal) spot spacing in the other direction. These results are consistent with a quasicrystalline material, and in particular, a decagaonal material. Decagonal quasicrystals are periodic in one dimension and aperiodic in the other two. However, the particular axis examined in the selected area diffraction patterns can be misleading; both the decagonal phase of this material and the orthorhombic approximant show very similar results according to the literature (1). Additional work in Phase II is needed to clarify this result.

Furthermore comparison of as-deposited and annealed PLD Al-Cu-Fe-Cr samples indicated that during annealing at 500°C for one hour Al-Cu-Fe-Cr grains grew from 10 nm (see Figure 7 report 8) to a size of about 100-1000 nm.

2.3.3 Nanohardness of Nanograins Al-Cu-Fe-Cr Coatings by Nanoindentation

An UMIS-2000 ultramicro-indentation system was used to investigate the hardness of the coatings. See Table 4. The UMIS-2000 uses a sharp Berkovich diamond (three-sided pyramid) indenter with a minimum force of 0.1mN. The depth resolution of the instrument is 1 nm. The instrument was calibrated using fused silica (hardness 9.5 GPa and elastic modulus 70 GPa). In this study, the maximum load was adjusted such that the maximum penetration depth corresponded to less than 10-15% of the coating thickness so that the influence of the substrate on the measurement can be neglected.[30] The force was incremented in 30 steps in a square root progression until the maximum load was achieved. This was followed by a hold segment of 100 sec to allow for relaxation of induced plastic flow and creep. Finally, the unloading segment was measured by decreasing the force. Typically, 10-12 indents were made for loads greater than 2 mN. For 2 mN loads, 40-50 indents were made to eliminate the noise at this low load. At low penetration depths, small deviations of the area function from a Berkovich diamond tip might cause errors in the absolute values of hardness and Young's modulus. The loading- unloading curves were averaged. This was used to determine the standard deviation in the maximum penetration depth. The data was analyzed using a MATHCAD computer program written at ACTG. The computer program analyzed the load-unloading curve based on the method of Oliver and Pharr.[30] The error in the hardness was evaluated from standard deviation in the penetration depth. The elastic contribution was determined from the unloading curve. From this the Young's modulus and plastic depth were determined. Figure 10 compares nanoindentation measurements for annealed-nanograins-PLD Al-Cu-Fe-Cr deposited on Si with large grain plasma spray Al-Cu-Fe-Cr. The increased hardness is due to reduction of grain size.

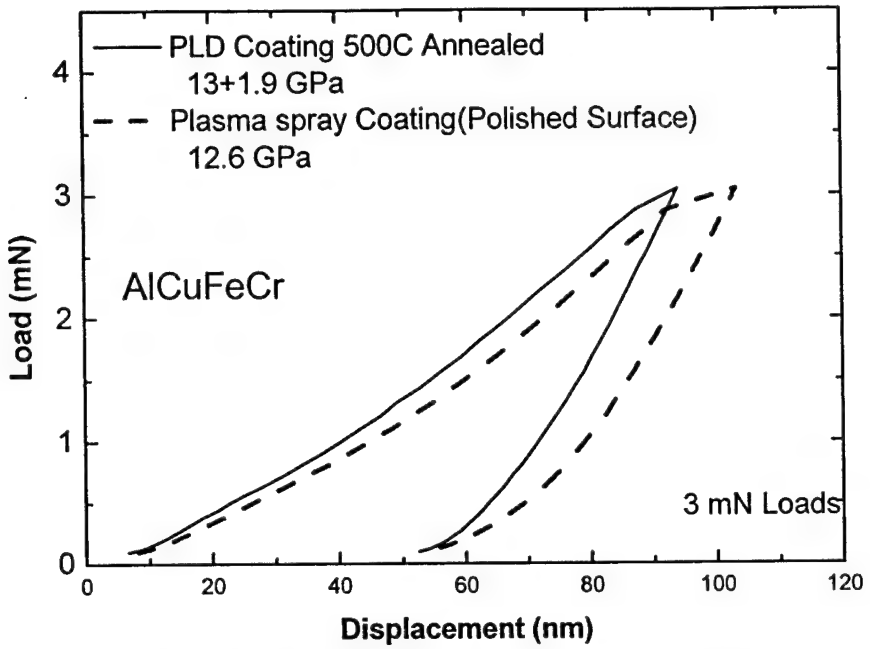

Figure 10 **Comparison of nanoindentation loading (3mN) and unloading curves for nanocrystalline AlCuFeCr film and polished plasma spray AlCuFeCr coating. Slightly higher hardness and less elastic deformation was observed for nanocrystalline AlCuFeCr.**

Table 4 **Characterization Results for Thin Film Samples of Al-Cu-Fe-Cr.**

Ames Lab #	Anneal	Load (mN)	Hardness (GPa)	Modulus (GPa)	EDS (at. %)
DJS-11-147	No	2 3 5	13±1.9 12±1.3 12.45±0.9	199 186 194	$Al_{62.6}Cu_{12.7}Fe_{10.8}Cr_{13.9}$
DJS-11-147-A	Yes	3 5	13.5±1.6 8.3±1.1	205 137	$Al_{64.1}Cu_{10.9}Fe_{10.9}Cr_{14.1}$
					$Al_{64.0}Cu_{10.8}Fe_{11.0}Cr_{14.2}$
					$Al_{63.1}Cu_{12.0}Fe_{10.7}Cr_{14.2}$
DJS-7-91-01	No	3 5	11.1±3.2 12.2±1.4	164 167.7	
DJS-10-5-A3	No	3 5	12.6 12.0	188 175.4	$Al_{60.9}Cu_{24.5}Fe_{13.1}Cr_{1.5}$
Bulk alloy	No	5 6 20	15±2 14±1.5 12±1.5	17 209 195	

2.3.4 Al-Cu-Fe

During the course of this program, Ames Laboratory shipped to Spire arc-melted coupons of composition $Al_{40}Cu_5Fe_{55}$. Specifically, these coupons were made from >99.99% pure elements by arc melting on a water-cooled copper hearth plate in an atmosphere of argon. This composition was chosen based upon published reports by researchers in Japan about the use of electron beam evaporation to produce quasicrystalline thin films.[26] A decreased amount of Al and Cu in the targets relative to the desired quasicrystalline composition of $Al_{63}Cu_{25}Fe_{12}$ is necessary to produce quasicrystalline films via this method because of the high vapor pressure of Al and Cu relative to Fe. In addition, if ion beams are used to produce films, one has to be careful because preferential sputtering of Al is known to occur.[27] We have performed a large number of IBAD runs to produce nanograin AlCuFe film.

Al-Cu-Fe Thin Film Analysis: We have shipped to Ames Laboratory six samples of Al-Cu-Fe deposited on silicon wafers. Table 5 summarizes the EDS and scanning electron microscopy results (Figures 11, 12, and 13) for the samples examined at Ames Laboratory. At Ames Laboratory, XRD was performed on all samples in the 2*theta region from 41 to 47°; within this region two peaks are expected for quasicrystalline samples of Al-Cu-Fe and one peak for crystalline materials. One sample showed two peaks in this region: DJS-12-113-D. All samples were subsequently heat treated at 500°C under vacuum. XRD results following heat treatment showed two peaks in the region from 41 to 47° **for DJS-12-113-C-A and DJS-12-113-D-**A. However, as shown in Table 5, the EDS results demonstrate that these samples are not corresponding to quasicrystalline as their compositions are far away from the quasicrystalline region of the Al-Cu-Fe phase diagram. Quasicrystalline Al-Cu-Fe has an approximate composition of $Al_{61.5\text{-}65}Cu_{23\text{-}30}Fe_{9\text{-}13}$.[13] Peaks for this system Table 6 are observed at 42.73° and 45.15° for Cu Kα radiation. For DWD-12-113-D peaks were observed at 43.45 and 44.44°. For DWD-12-113-C-A peaks were seen at 43.02 and 44.73°. For DWD-12-113-D-A peaks were seen at 42.59 and 44.30°. The origin of these peaks is not known at this time. Although, peak 1 for sample DWD-12-113-D-A in Table 6 similar to that reported for quasicrystals Al-Cu-Fe. Furthermore, nanohardness of this sample shows a hardness of about 14 GPa, see Table 7. Considering nanohardness and X-ray data we speculate that sample **DJS-12-113-D-A** consisted of AlCuFe quasicrystals and Fe materials, which should be carefully investigated in the Phase II program.

Table 5 **Summary of EDS and SEM Results for Thin Film Samples of Al-Cu-Fe.**

Spire Sample #	Ames Lab #	Rate/ Beam Current/ Temp	Heat Treated ?	EDS (at. %)	SEM Comments
200110209	DJS-12-113-A	6/100/RT	No	$Al_{25.8}Cu_{4.1}Fe_{70.4}$	100 nm long particles
	DJS-12-113-A-A	6/100/RT	Yes	$Al_{39.2}Cu_{6.9}Fe_{53.9}$ $Al_{38.7}Cu_{7.1}Fe_{54.2}$ $Al_{38.6}Cu_{7.5}Fe_{53.9}$	Significant spalling < 50 nm particle size
200103109	DJS-12-113-B	3/100/RT	No	$Al_{16.7}Cu_{2.7}Fe_{80.6}$	200 nm long particles
	DJS-12-113-B-A	3/100/RT	Yes	$Al_{29.7}Cu_{4.5}Fe_{68.8}$ $Al_{30.1}Cu_{4.4}Fe_{65.5}$	0.25 um holes * 300 nm long particles
400071702	DJS-12-113-C	3/0/RT	No	$Al_{0.2}Cu_{0}Fe_{0}Cr_{99.8}$	
	DJS-12-113-C-A	3/0/RT	Yes	$Al_{0.7}Cu_{0.1}Fe_{0}Cr_{99.2}$	50-100 nm particles
200103009	DJS-12-113-D	3/50/RT	No	$Al_{26.2}Cu_{4.2}Fe_{69.6}$	< 50 nm particle size
	DJS-12-113-D-A	3/50/RT	Yes	Film spalled off	
200111609	DJS-12-113-E	6/50/322C	No	$Al_{13.6}Cu_{0.5}Fe_{85.9}$	150-200 nm particle size
	DJS-12-113-E-A	6/50/322C	Yes	$Al_{23.0}Cu_{1.1}Fe_{75.9}$	Cracking, 150-200 nm particle size
200110709	DJS-12-113-F	6/100/210C	No	$Al_{18.1}Cu_{1.2}Fe_{80.7}$ $Al_{18.1}Cu_{1.2}Fe_{80.7}$	100 nm particles
	DJS-12-113-F-A	6/100/210C	Yes	$Al_{34.3}Cu_{4.5}Fe_{61.2}$	Cracking, 200 nm holes
	DJS-11-147	PLD	No	$Al_{62.6}Cu_{12.7}Fe_{10.8}Cr_{13.9}$	1-20 um particles
	DJS-11-147-A		Yes	$Al_{64.1}Cu_{10.9}Fe_{10.9}Cr_{14.1}$ $Al_{64.0}Cu_{10.8}Fe_{11.0}Cr_{14.2}$ $Al_{63.1}Cu_{12.0}Fe_{10.7}Cr_{14.2}$	1-20 um particles
	DJS-10-5-A3	Plasma spray	No	$Al_{60.9}Cu_{24.5}Fe_{13.1}Cr_{1.5}$	30 um particles

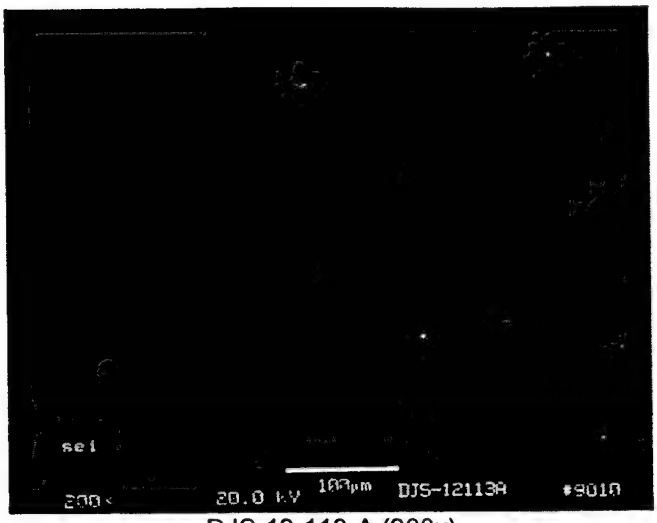

DJS-12-113-A (200x)

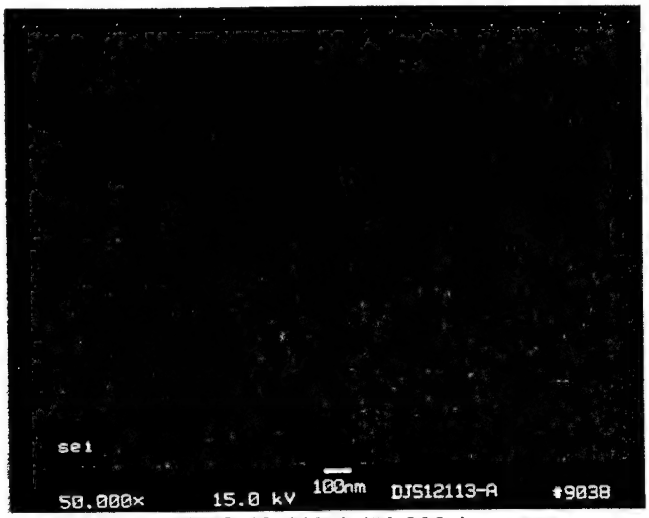

DJS-12-113-A (50,000x)

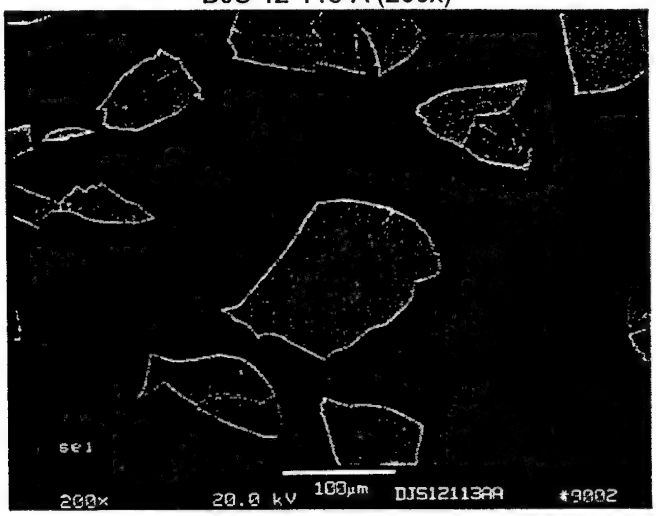

DJS-12-113-A-A (200x)

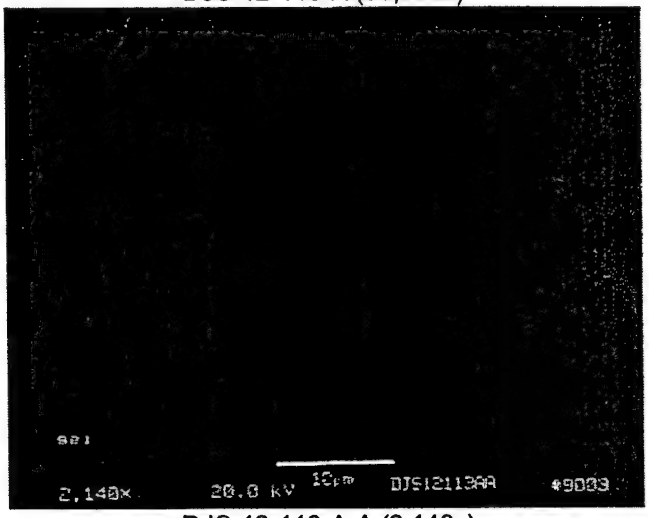

DJS-12-113-A-A (2,140x)

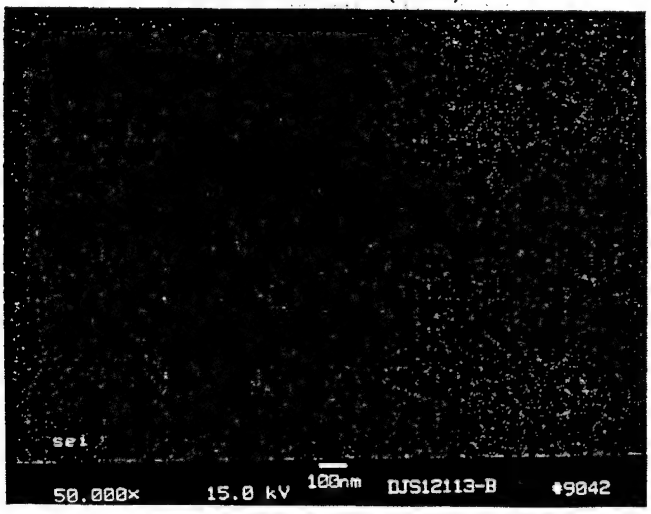

DJS-12-113-B (50,000x)

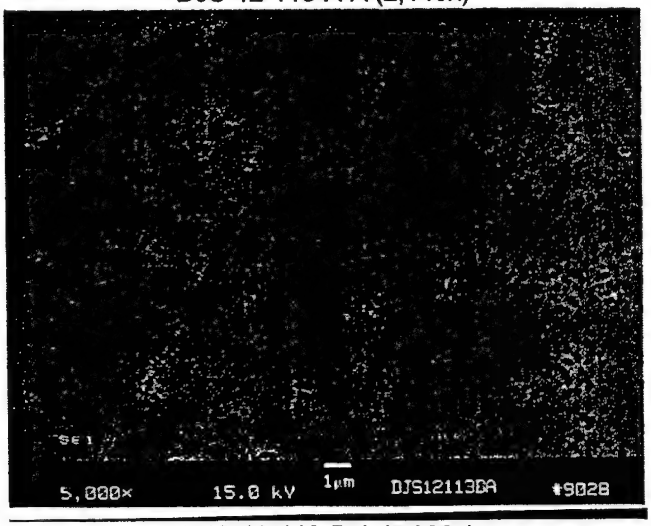

DJS-12-113-B-A (5,000x)

Figure 11 SEM results for thin films of Al-Cu-Fe produced by IBAD.

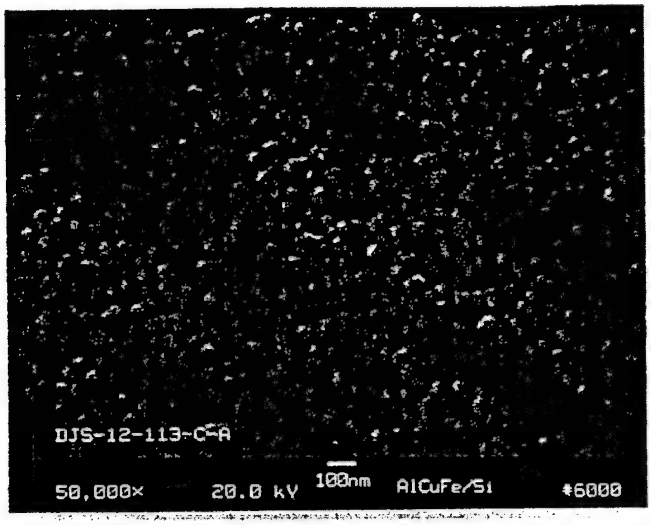

DJS-12-113-C-A (50,000x)

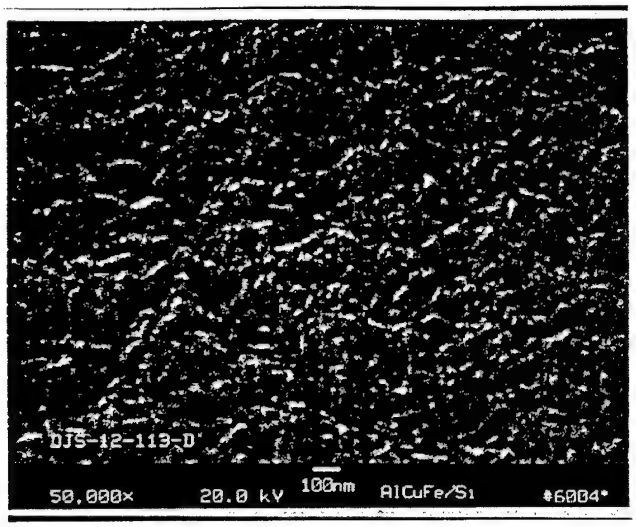

DJS-12-113-D (50,000x)

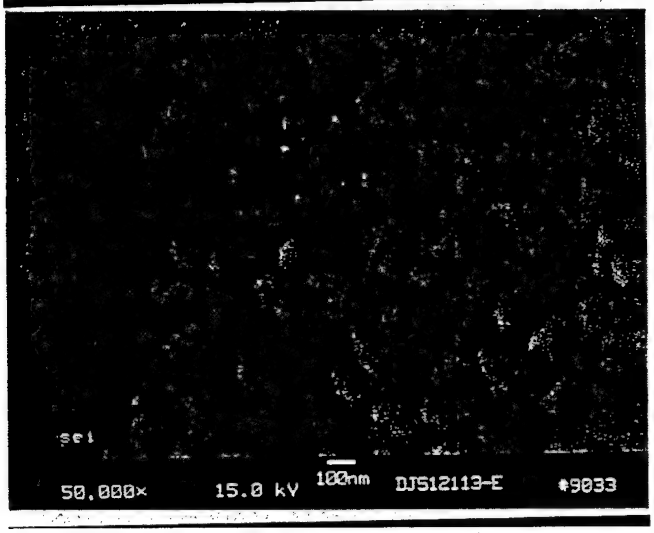

DJS-12-113-E (50,000x)

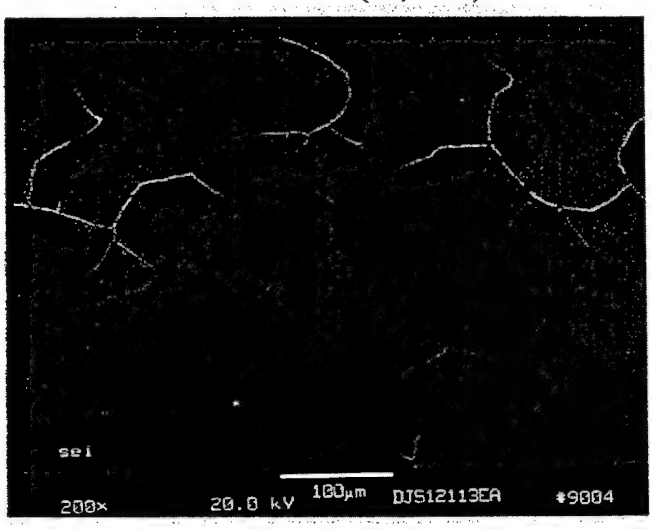

DJS-12-113-E-A (50,000x)

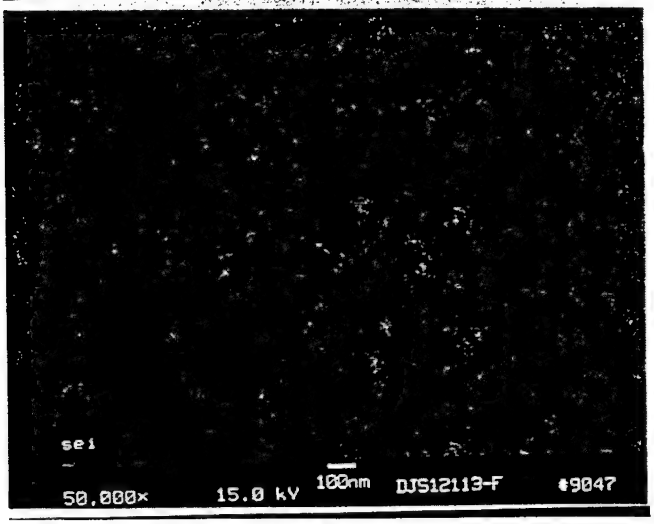

DJS-12-113-F (50,000x)

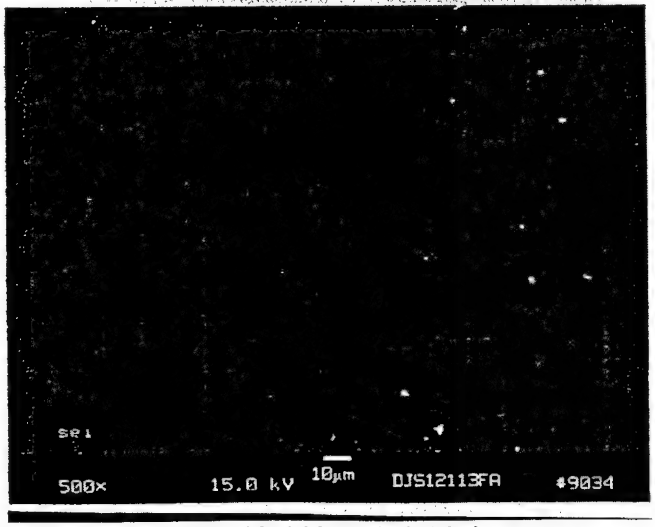

DJS-12-113-F-A (500x)

Figure 12 SEM results for thin films of Al-Cu-Fe continues

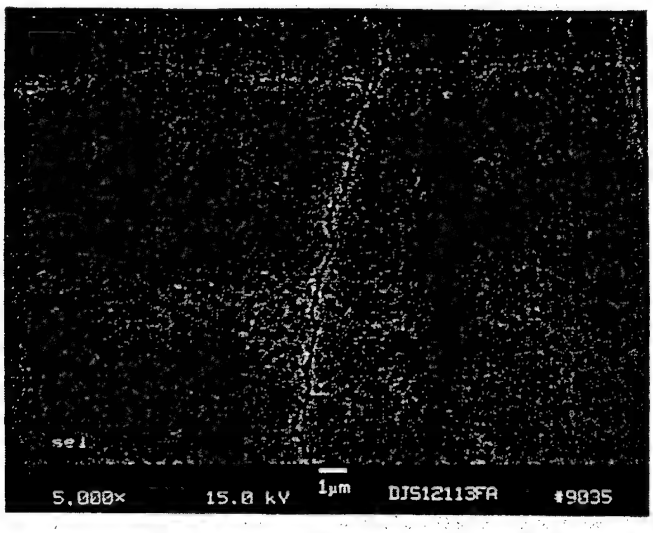

DJS-12-113-F-A (5,000x)

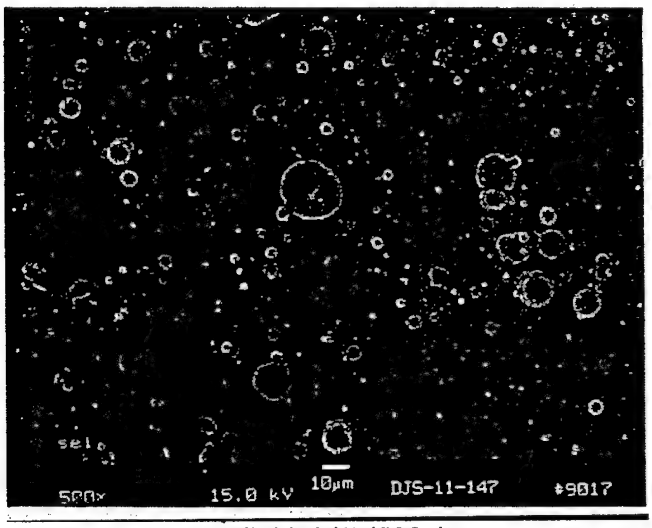

DJS-11-147 (500x)

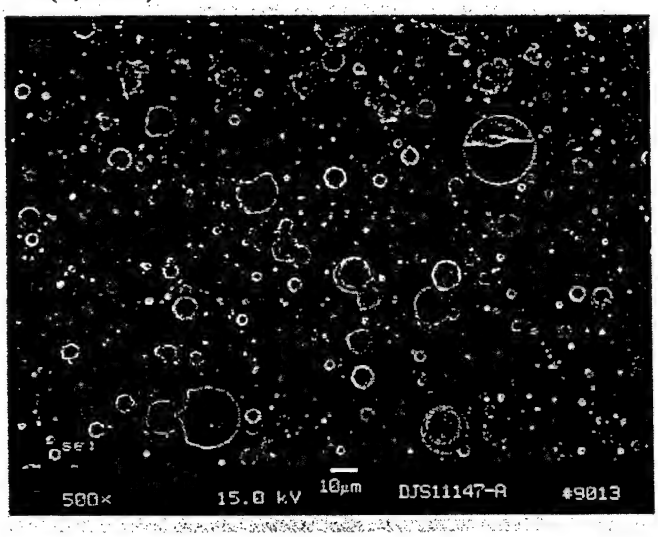

DJS-11-147-A (500x)

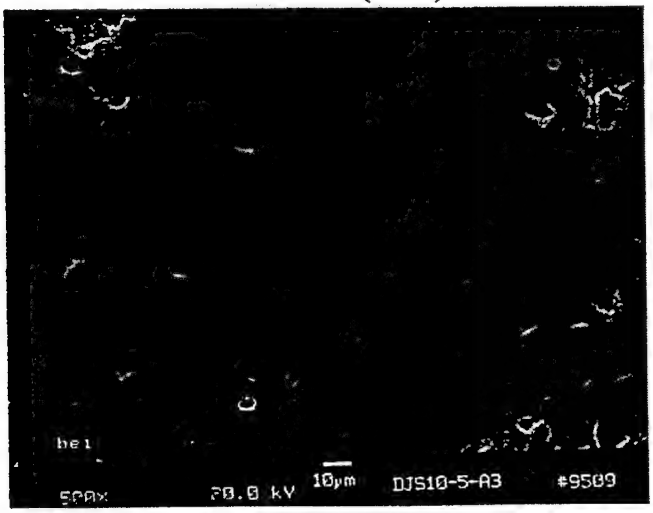

DJS-510-5-A3 (500x)

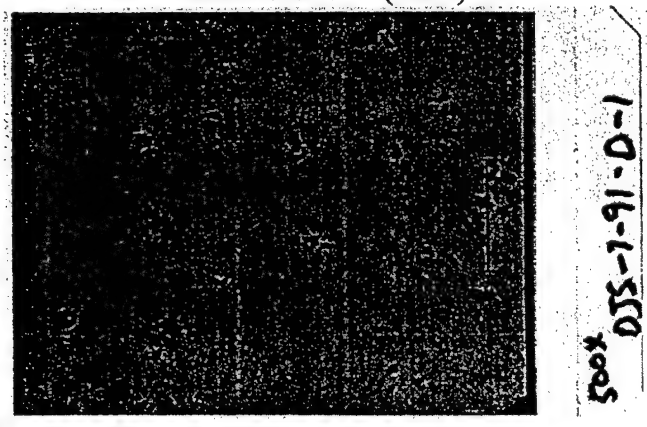

DJS-7-91-D-1 (500x)

Figure 13 SEM results for thin films of Al-Cu-Fe continues.

Table 6 **X- ray diffraction peaks from Al-Cu-Fe thin films samples.**

Ames Lab Sample #	Peak 1	Peak 2
From literature For AlCuFe	42.73°	45.15°
DWD-12-113-D	43.45°	44.44°
DWD-12-113-D-A	42.59°	44.30°.
DWD-12-113-C-A	43.02°	44.73°

Table 7 **Nanohardness results for thin film samples of Al-Cu-Fe.**

Spire Sample #	Ames Lab #	Anneal 500 C	Load (mN)	Hardness (GPa)	Modulus (GPa)
200103009	DJS-12-113-D	No	2 3 5	9.5±1.6 9.8±2.2 8.6±0.7	188.3 188 169
	DJS-12-113-D-A	Yes	3 5	13.9±0.95 13.6±0.6	176 172
200111609	DJS-12-113-E	No	2 3 5	12.7±2.9 12.3±0.9 10.9±0.9	200 191 177
	DJS-12-113-E-A	Yes	3 5	7.96±1.2 6.8±0.7 Surface	165 151 cracked
200110709	DJS-12-113-F	No	2 3 4 5	10.1±1.3 8.99±0.5 10.1±1 10.3±2	211 198 187 183
	DJS-12-113-F-A	Yes	3 5	Cracked 6.1±0.8	Surface 152

3. CONCLUSION

In phase 1 program Ion-Beam Assisted Deposition (IBAD) and Pulsed laser Deposition (PLD) applied to deposit nanograin Al-Cu-Fe and Al-Cu-Fe-Cr films respectively. Al-Cu-Fe and Al-Cu-Fe-Cr quasicrystals targets materials produced at Ames Laboratory. Al-Cu-Fe and Al-Cu-Fe-Cr quasicrystals films studied at Ames Laboratory as well as Spire Corporation. Our results as shown by TEM, indicated fabrication of ultra-smooth Al-Cu-Fe-Cr for samples produced by PLD. The grain size for as deposited Al-Cu-Fe-Cr is about 10 nm and for annealed samples (500C) is less than one micron. Both RBS and EDS shown the composition of coated Al-Cu-Fe-Cr samples are similar to the source materials, which were provided by Ames Laboratory. Nanohardness of annealed Al-Cu-Fe-Cr samples were about 13 GPa. X-ray analysis by Ames Laboratory suggested that the coatings of Al-Cu-Fe-Cr produced are quasicrystalline in nature although an orthorhombic approximant cannot be ruled out by the data presented here.

Based upon published reports by researchers in Japan about the use of electron beam evaporation to produce quasicrystalline $Al_{63}Cu_{25}Fe_{12}$ thin films and because of time and funding limitations impose by phase 1, $Al_{40}Cu_5Fe_{55}$ composition was chosen as a source materials for e-beam evaporation. The Al-Cu-Fe thin films produced by IBAD using $Al_{40}Cu_5Fe_{55}$ as a source materials where substantially depleted in Al and enriched in Fe relative to the composition region in which quasicrystals can be produced in this system. Nevertheless Al-Cu-Fe thin films are very smooth and hard and consist of grains with 10 to 50 nm and posses a nanohardness of 14 GPa. There are indications that suggesting our AlCuFe samples are consisted of quasicrystals of AlCuFe and iron alloys. Phase II will apply TEM analysis these samples to verify possibility of to formation multi-phase AlCuFe quasicrystals and metallic crystalline phases.

REFERENCES

1. D. Shechtman, I. Blech, D. Gratias and J.W. Cahn, Phys. Rev. Lett. 53 (1984) 1951-1953.
2. K.F. Kelton, Int. Mater. Rev. 38 (1993) 105-137.
3. A.I. Goldman and M. Widom, Annu. Rev. Phys. Chem. 42 (1991) 685-729.
4. P.W. Stephens and A.I. Goldman, Scientific American (April 1991) 24-31.
5. C.J. Jenks and P.A. Thiel, Langmuir 14 (1998) 1392-1397.
6. J.-M. Dubois, P. Brunet and E. Belin-Ferré, in: Current Topics in Quasicrystals, Eds. E. Belin-Ferré, C. Berger, M. Quiquandon and A. Sadoc (World Scientific, Singapore, 2000) pp. 498-532.
7. J.M. Dubois, A. Proner, B. Bucaille, P. Cathonnet, C. Dong, V. Richard, A. Pianelli, Y. Massiani, S. Ait-Yaazza and E. Belin-Ferre, Ann. Chim. Fr. 19 (1994) 3-25.
8. O.G. Symko, W. Park and D. Kieda, in: Surface Modification Technologies XI, Eds. T.S. Sudarshan, M. Jeandin and K.A. Khor (The Institute of Materials, London, 1998) pp. 1051-1056.
9. P.C. Gibbons and K.F. Kelton, in: Physical Properties of Quasicrystals, Ed. Z.M. Stadnik (Springer-Verlag, Berlin, 1999) pp. 403-431.
10. Y. Massiani, S. Ait Yaazza and J.-M. Dubois, in: Proceedings of the 5th International Conference on Quasicrystals, Eds. C. Janot and R. Mosseri (World Scientific, Singapore, 1995) pp. 790-793.
11. J.-M. Dubois, S.S. Kang and Y. Massiani, J. Non-Cryst. Solids 153/154 (1993) 443-445.
12. A.I. Goldman and K.F. Kelton, Rev. Modern Phys. 65 (1993) 213-230.
13. F.W. Gayle, A.J. Shapiro, F.S. Biancaniello and W.J. Boettinger, Metallurgical Transactions A 23A (1992) 2409-2417.
14. D.J. Sordelet, S.D. Widener, Y. Tang and M.F. Besser, Mater. Sci. Engr. A A294-296 (2000) 834-837.
15. I.M. Hutchings, Tribology: Friction and Wear of Engineering Materials (CRC Press, Boca Raton, FL, 1992).
16. R.H. Perry and C.H. Chilton, Eds., Chemical Engineers' Handbook (McGraw-Hill, New York, 1973).
17. J.M. Dubois and P. Weinland, USA Patent 5,204,191, Coating Materials for Metal Alloys and Metals and Methods (1993).
18. U. Köster, W. Liu, H. Liebertz and M. Michel, J. Non-Cryst. Solids 153/154 (1993) 446-452.
19. S.S. Kang, J.M. Dubois and J. von Stebut, J. Mater. Res. 8 (1993) 2471-2481.
20. J.-M. Dubois, S.S. Kang and A. Perrot, Mater. Sci. Engr. A 179/180 (1994) 122-126.
21. J. Lyons and T. Starr, J. Am. Ceram. Soc. 77 (1994) 1673-1675.
22. H.E. Boyer and T.L. Gall, Eds., Metals Handbook (American Society of Metals, Metals Park, OH, 1985).
23. P. Archambault, in: New Horizons in Quasicrystals: Research and Applications, Eds. A.I. Goldman, D.J. Sordelet, P.A. Thiel and J.-M. Dubois (World Scientific, 1997) pp. 224-231.
24. D.J. Sordelet, M.J. Kramer and O. Unal, J. Thermal Spray Tech. 4 (1995) 235-244.
25. C. Dong and J.M. Dubois, J. Mater. Sci. 26 (1991) 1647-1654.
26 A. Yoshioka, K. Edagawa, K. Kimura and S. Takeuchi, Jpn. J. Appl. Phys. 34 (1995) 1606-1609.
27 .J. Jenks, J.W. Burnett, D.W. Delaney, T.A. Lograsso and P.A. Thiel, Appl. Surf. Sci. 157(2000) 23-28.

28. J. A. Greer, M.D. Tabat, and C. Lu, "Future Trends for Large-Area Pulsed Laser Deposition," Nuclear Instruments and Methods in Physics Research, **B** 121, pp. 357-362, 1997.
29 M.F. Besser and T. Eisenhammer, MRS Bull. 22 (1997) 59-63
30. W. C. Oliver and G. M. Pharr, J. Mater. Res. 7, 1564 (1992).